A PRO-RESOLVING LIPID MEDIATOR FOR THE ATTENUATION OF OSTEOARTHRITIS PATHOLOGY

by

EMILY SVERDRUP

A THESIS

Presented to the Department of Chemistry
and the Robert D. Clark Honors College
in partial fulfillment of the requirements for the degree of
Bachelor of Science

April 2025

An Abstract of the Thesis of

Emily Sverdrup for the degree of Bachelor of Science
in the Department of Chemistry to be taken June 2025

Title: A Pro-Resolving Lipid Mediator for the Attenuation of Osteoarthritis Pathology

Approved: *Nick Willett, Ph.D.*
Primary Thesis Advisor

Osteoarthritis (OA) is a chronic joint disease characterized by pain and impaired joint mobility; OA currently has no cure and there are no FDA-approved drugs on the market for the treatment of OA. The chronic nature of OA is associated with an unresolved, localized inflammatory immune response. Resolvin D1 (RvD1) is an endogenous pro-resolving lipid mediator, produced in response to inflammation, that promotes inflammation resolution and tissue regeneration. This work tests the effect of RvD1 as a therapeutic for OA *in vitro* in macrophages and in a preliminary preclinical animal model after a non-invasive anterior cruciate ligament rupture (ACLr). Murine RAW 264.7 macrophages were treated with RvD1 for 24-hours then stimulated with lipopolysaccharides and co-treated with RvD1. After 4-hours, the cells were fixed and stained for intracellular TNF-α. The media was collected and analyzed for nitrite content. Male Lewis rats (n=3-6/group) received either ACLr or a Sham procedure, followed by intra-articular injection of saline, RvD1 (100 ng), or RvD1 loaded into polyethylene glycol microgels. Knee joint structural changes were quantified via contrast-enhanced μCT post-mortem and functional effects were analyzed via Bioseb Dynamic Weight Bearing assay. RvD1 showed no significant effect on TNF-α and nitrite activity, although the immortalized cell line may have altered RvD1 binding. *In vivo*, RvD1 significantly improved articular cartilage attenuation (a proxy for cartilage quality) and reduced cartilage erosion.

Further experiments are needed to fully power these findings. This preliminary work suggests that Resolvin D1 may have potential as a treatment for osteoarthritis and further research is essential to fill the current gap in care.

Acknowledgements

I would like to thank my primary thesis advisor, Dr. Nick Willett, for his consistent support and guidance throughout my time in the lab. My experiences in the Willett lab have broadened my appreciation for research exponentially and have exposed me to so many amazing opportunities both in the lab and beyond. I would like to offer a special thank you to Nicholas Pancheri, my graduate student advisor who has been there every step of the way since Day 1 in the lab. I would also like to thank the members of the Willett and Guldberg labs who have supported this work along the way: Frank Pittman, Sruthi Ranganathan, Kait Link, and Angela Lin to name just a few. I would also like to thank my CHC representative, Dr. Lindsay Hinkle, who not only inspires my love of science but has been a wonderful teacher over my years in the Clark Honors College. Finally, I would like to thank my mom, Dr. Eileen Sverdrup, for her boundless love and support. I would not be where I am without her. This work was supported by the Hui Undergraduate Scholars Program and the Undergraduate Research Opportunity Program in the Office of the Vice President for Research and Innovation.

Table of Contents

List of Figures

Introduction

Osteoarthritis (OA) is the most common form of arthritis and affects ~27 million people with healthcare costs that exceed $185 billion annually in the US alone.[1] OA is a degenerative joint disease, known as the "wear and tear" disease, and manifests as chronic pain and impaired joint mobility in advanced disease stages. Such OA indications encourage low mobility lifestyles which increase risks for diabetes and cardiovascular disease.[2,3] OA has no cure and there are no disease-modifying FDA-approved drugs currently on the market. Treatment is limited to symptom management, commonly in the form of pain relievers and anti-inflammatories, typically NSAIDs, and prescribed physical rehabilitation which produces highly variable outcomes and suffers from poor patient compliance.[4] In recent years, numerous prospective therapies have been researched for intra-articular injection of potential disease-modifying drugs but have failed to translate to positive clinical outcomes. One such drug of interest is Resolvin D1, a pro-resolving lipid mediator thought to mediate the chronic inflammatory immune response associated with OA disease progression. The therapeutic efficacy of potential OA disease-modifying drugs is believed to be limited by rapid drug degradation and removal from the joint tissue. A solution to the poor retention and bioavailability of the drug within the joint space is a sustained drug delivery system. Common approaches utilize micro- and nano-carrier structures (e.g., nanoparticles, liposomes, and hydrogels) that act as drug delivery vessels for sustained bioavailability.

An indication of OA pathology is chronic inflammation, which causes cartilage degeneration, pain, and reduced limb function. Specialized pro-resolving mediators are lipid molecules that are produced naturally from tissue injury; they discourage over-reaction by the immune system and stimulate resolution of the inflammatory response.[5] Chronic activation of the

inflammatory macrophage state is thought to be a major contributor to OA-related inflammation. Macrophages are a type of white blood cell that contributes to the function of the innate immune system via paracrine signaling (e.g., secreted proteins known as cytokines). Macrophages exist in one of two states: the classically activated M1 state, which produces pro-inflammatory cytokines, and the alternatively activated M2 state, which produces anti-inflammatory cytokines and is associated with tissue repair and wound healing.[6] Delivery of specialized pro-resolving mediators, such as the molecule Resolvin D1 (RvD1), may be used therapeutically to supplement endogenously produced specialized pro-resolving mediators and control the immune response after joint injury or in response to excessive wear and tear.[5] Specialized pro-resolving mediators are hypothesized to work by blunting M1 macrophage proinflammatory cytokine production and promoting the transition to and the upregulation of the M2 anti-inflammatory state. Specialized pro-resolving mediators are an exciting avenue for application within a sustained drug delivery system to regulate and potentially reverse OA disease progression.[6]

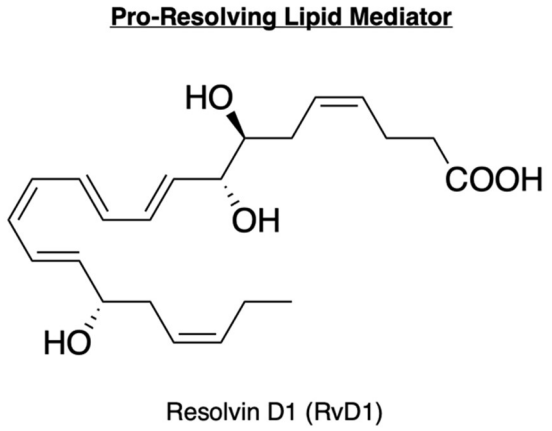

Figure 1: Resolvin D1 (RvD1) molecular structure. RvD1 is derived from polyunsaturated omega-3 fatty acids through enzymatic reductions.

The mechanism of action of RvD1 was explored *in vitro* via macrophage cell culture. In this experiment, RAW 264.7 macrophages were treated with increasing doses of RvD1 then

stimulated to the M1 inflammatory state with lipopolysaccharides. RAW 264.7 is a macrophage cell line isolated from a tumor in a male mouse induced with the Abelson murine leukemia virus and is widely used in drug development research.[7] Lipopolysaccharides (LPS) are an outer membrane component of Gram-negative bacteria that induces inflammatory cytokine secretion (including IL-1, IL-6, and TNF-α) and nitrite production in macrophages.[8] Quantifying the relative production of TNF-α and nitrite with RvD1 treatment in a macrophage stimulation model is a promising avenue for quantifying the immunomodulatory effects of RvD1.

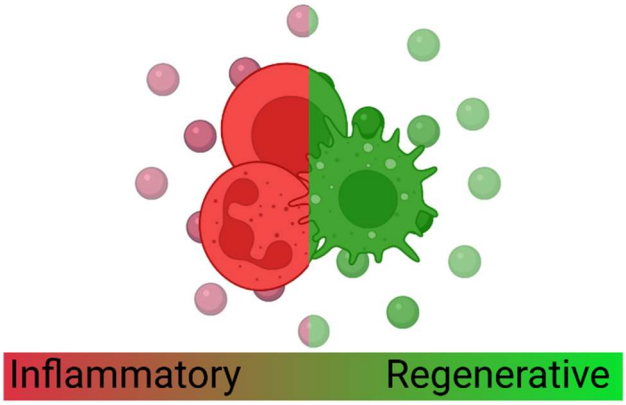

Figure 2: Macrophage polarization between an inflammatory (M1) state and an anti-inflammatory, regenerative (M2) state (figure made in Biorender.com).

For the *in vivo* characterization of Resolvin D1, a representative animal model of osteoarthritis was needed. The current standard in the field is to perform a medial meniscal transection (MMT) surgery on a rat model to induce a form of post-traumatic, or post-injury, osteoarthritis (PTOA). MMT surgery causes joint instability and catabolic tissue phenotypes like clinical PTOA pathologies; however, surgical induction causes a confounding inflammatory immune response. Our studies utilize a non-invasive anterior cruciate ligament (ACL) injury model which may better represent the injury induction mode and inflammatory state in humans. In this model, an axial force is applied to the knee joint that ruptures the ACL, causing joint instability and osteoarthritis pathology comparable to MMT. The non-invasive ACL injury

model is also highly representative of naturally occurring ACL injuries which exhibit PTOA initiation rates as high as 87%.[12] When introducing a drug to an injury site such as the joint space with high clearance rates, identifying a method of encapsulation for sustained drug delivery may be valuable.

Nanoparticles can be engineered from a wide variety of materials and are defined by their 1 nm to 100 nm size (similar to the size of DNA and viruses). Due to their nano-scale architecture, nanoparticles can penetrate normally inaccessible regions, be functionalized to target different tissues and environments, and increase the aqueous solubility of carried drugs.[9] In OA specifically, nanoparticles are small enough to diffuse through layers of cartilage, thereby increasing drug bioavailability.[10] Both liposomes and hydrogels can be scaled down to the nano-particle level; however, at that scale, they are quickly cleared with the lymphatic fluid through microcirculation in the synovial membrane. Liposomes are spherical vesicles made of phospholipids that condense to form a lipid bilayer, which have been explored extensively and are established drug delivery vessels. Liposomes make effective drug carriers because they have high biocompatibility, are relatively easy to make, and can carry both hydrophobic and hydrophilic loads. However, liposome encapsulation techniques can be limited by poor loading efficiency or undesirable release kinetics; this in conjunction with their rapid clearance rates rationalizes research into alternative delivery methods.

Hydrogels are crosslinked polymeric spheres with high biocompatibility and easily modifiable size and crosslink density; microgels are hydrogels that range from one to several hundred micrometers in size. Microgels can be fabricated from a variety of both natural and synthetic polymers. While natural polymers have advantages in their high biocompatibility and biodegradability, synthetic polymers such as polyethylene glycol (PEG) are valuable because

they are also biocompatible, their binding affinity and physicochemical properties are tunable, and the consistency and purity of the polymer is more reliable (which is desirable for clinical translation). An oil-in-water emulsion system with an engineered microfluidic chip has demonstrated successful drug encapsulation and production of PEG microgels with relatively uniform size, and the PEG microgels elicit higher drug retention rates in the joint space compared to freely injected drug.[11] Outcomes of this methodology justify further use of this approach in our own work. Microgels do have limitations surrounding their drug loading capacity and release kinetics similar to liposomes and cannot be stored loaded. This poses logistical challenges particularly in a clinical setting, although lyophilization (i.e., freeze-drying) may be developed to improve shelf stability and post-fabrication drug loading.

We hypothesized that drug-loaded, covalently crosslinked PEG microgels would increase joint retention times compared to freely injected drug, thereby enhancing therapeutic effects and improving treatment homogeneity. Our objective was to evaluate the immunomodulatory effects of Resolvin D1 *in vitro* and investigate the ability of free and encapsulated Resolvin D1 to attenuate osteoarthritis pathology in a preclinical rodent model of post-traumatic osteoarthritis. We intended to assess the cartilage morphometric changes and functional therapeutic effects of intra-articular injection of free versus encapsulated RvD1 treatment *in vivo*. Subsequent preclinical testing will inform future studies to identify if this is a clinically relevant intervention with the potential to improve patient quality of life.

Methods

In Vitro Resolvin D1 Characterization

Macrophage Cell Culture

RAW 264.7 macrophages were cultured in a 96-well plate at 10,000 cells per well in DMEM (Dulbecco's Modified Eagle Medium) GlutaMAX high glucose media. There were six groups: a media only control, an LPS stimulation control, three RvD1 unstimulated treatment groups and three RvD1 stimulated treatment. The cells were left to incubate for 16 to 18 hours at 37 °C. The RvD1 treatment groups were pretreated with 5, 10, and 50 ng/mL RvD1 for low-dose experiments and 50, 100, and 500 ng/mL for high-dose experiments. Non-treatment groups received a normal media change. After 24 hours in 37 °C incubation, all cells were treated with Brefeldin A, a protein transport inhibitor that enhances intracellular protein visualization post-staining. Stimulated groups were treated with 50 ng/mL of lipopolysaccharides and treatment groups received their corresponding dose of RvD1. After 4 hours, the cell media was collected, and the macrophages were fixed with 4% paraformaldehyde. Experiments were repeated one to three times (three low-dose replicate experiments and one high-dose experiment).

Intracellular TNF-α Staining

The fixed RAW 264.7 macrophages were washed with phosphate-buffered solution (PBS) and then permeabilized with 0.1% Triton-X in PBS. Permeabilization makes the cell membrane more porous, making the intracellular proteins accessible for staining. A blocking buffer of 0.1% bovine serum albumin (BSA) weight per volume in PBS was applied to prevent the non-specific binding of antibodies. The cells were treated with Rabbit Anti-TNFα antibody, incubated at 4 °C overnight, then treated with Goat Anti-Rabbit IgG H&L at room temperature

for an hour. Finally, the cells were stained with DAPI (4′,6-diamidino-2-phenylindole) nuclei stain for two minutes. The stains were visualized and imaged on a fluorescent microscope with DAPI and Texas Red filters at x10 magnification. Each well was imaged in two locations and the resulting data from the technical replicates were averaged to produce one data point per well.

ImageJ Image Analysis

The stained cells were imaged with the DAPI and Texas Red filters then uploaded to the ImageJ software for image analysis. In ImageJ, the number of nuclei stained by the DAPI stain were quantified to determine cell count. This was done with the "Nuclei Count" script shown below. We employed two methods for quantifying the TNF-α stain. The "% Area" script isolates the red of the TNF-α stain and determines how much of the picture is red versus not. The "Mean Grey" script accounts for the intensity of the TNF-α stain by assigning the red pixels an intensity value then taking the average. The background was subtracted to minimize the significance of off-target staining in our data. Both % Area and Mean Grey data were normalized to the nuclei count.

Nuclei Count:

```
Count Nuclei
run("Split Channels");
setAutoThreshold("Default dark");
//run("Threshold...");
setThreshold(20, 255, "raw");
//setThreshold(20, 255);
setOption("BlackBackground", true);
run("Convert to Mask");
run("Despeckle");
run("Fill Holes");
run("Watershed");
run("Analyze Particles...", "size=40-1000 show=Masks clear summarize");
```

% Area:

```
run("Split Channels");
close();
close();
setAutoThreshold("Default dark");
//run("Threshold...");
setThreshold(23, 255, "raw");
//setThreshold(23, 255);
setOption("BlackBackground", true);
run("Convert to Mask");
run("Set Measurements...", "area area_fraction display redirect=None decimal=3");
run("Measure");
close();
```

Mean Grey:

```
run("Split Channels");
close();
close();
run("Subtract Background...", "rolling=50");
run("Set Measurements...", "area mean display redirect=None decimal=3");
run("Measure");
close();
```

Measure-It High Sensitivity Quantization Assay

Nitrite is a byproduct of nitric acid; nitric acid is produced via the inducible nitric oxide synthase (iNOS) cycle which is stimulated by inflammatory signals. As such, nitrite content can be measured as a proxy for inflammation. The Measure-iT™ (ThermoFischer) nitrite quantitation standard was used to make 0 to 55 μM concentrations of nitrite. The Measure-iT™ nitrite quantitation reagent was diluted then aliquoted into wells of a black 96-well plate. 2 μL of each nitrite standard were added in duplicate and 10 μL samples of the isolated media from the macrophage cell culture experiments were added in duplicate to the well plate. The well plate was incubated at room temperature for 10 minutes then Measure-iT™ nitrite quantitation

developer was added. The fluorescence was measured using a plate reader covering the excitation and emission maxima range of 365 to 450 nm.

In Vitro Microgel Fabrication and Quantization

Microfluidic Chip Fabrication

Silicon wafers were etched with the channel layout of the desired chips using a photomask and photolithography. The channels were cast into polydimethylsiloxane (PDMS) chips using the silicon wafers as a mold via soft lithography. The PDMS chips were then bonded to glass microscope slides with a plasma coater to form sealed channels. The channel sizes were preselected to produce 70 μm gels. All fabrication steps were completed either in a clean room or chemical hood to minimize debris in the channels. The chips were examined under a brightfield microscope to verify successful fabrication.

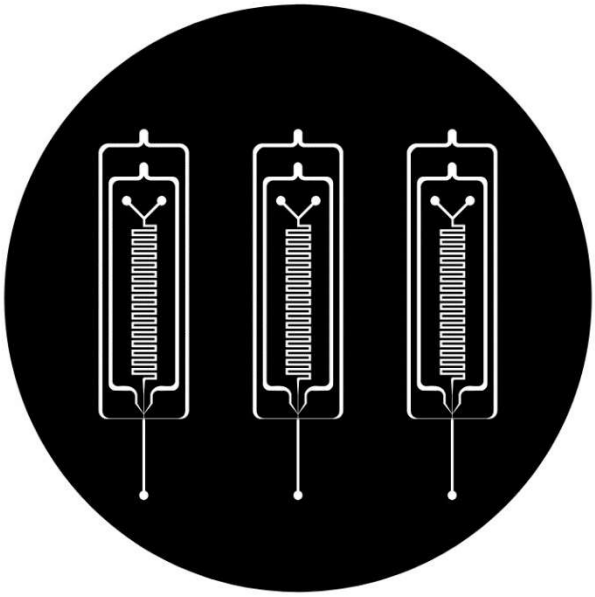

Figure 3: Photomask for silicon wafer etching of microfluidic chips.

Microgel Fabrication

Flow-focusing microfluidic geometry directs the formation of polymer spheres. First, mineral oil was flushed through the chip to clear and prime the channels. The crosslinker phase is a combination of mineral oil, 2% SPAN80, and a 1:15 ratio of 20 mg/mL dithiothreitol (DTT) crosslinker. The polymer phase contains 5% PEG-4MAL with the drug to be encapsulated. The water in oil emulsion directed by the microfluidic geometry of the chip produced 70 μm crosslinked PEG microgels which were collected in a tube of bovine serum albumin (BSA), washed by centrifugation, then frozen down in 300 μL aliquots at–80 °C.

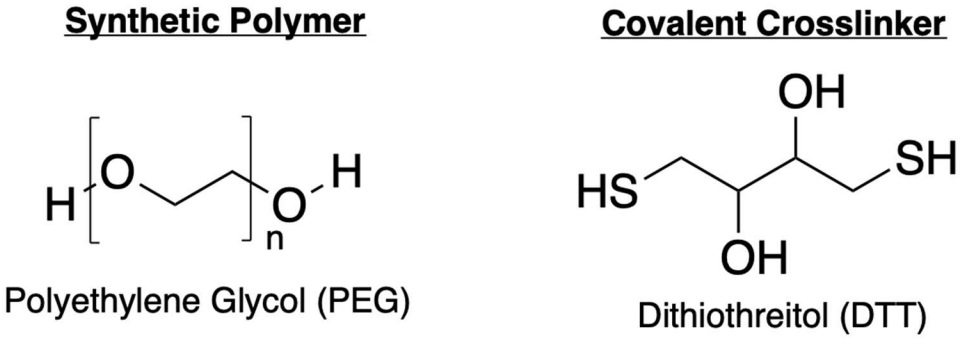

Figure 4: Molecular structure of polyethylene glycol polymer and dithiothreitol crosslinker.

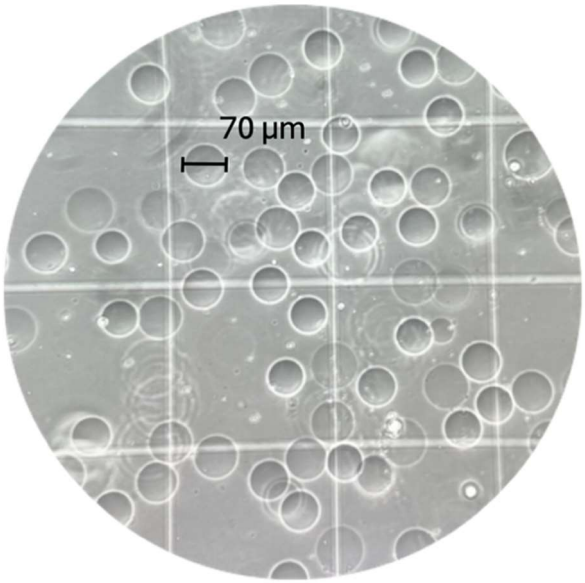

Figure 5: Brightfield image of PEG microgels in hemocytometer. Scale bar = 70 µm.

Enzyme Linked Immunosorbent Assay

Enzyme-Linked Immunosorbent Assays (ELISA) are kits tailored to the molecule or protein of choice. For our *in vitro* and *in vivo* characterization experiments, we used the 17(R)-Resolvin D1 isomer; however, due to a lack of commercial availability of a 17(R)-Resolvin D1 ELISA assay, for our drug release time course we used 17(S)-Resolvin D1. Following fabrication, 17(S)-Resolvin D1 loaded microgels in BSA were stored at either 4 °C or 37 °C for 1-, 4-, 18-, 24-, and 48-hour timepoints. The aliquots were then centrifuged, and the supernatant was removed and stored at -80 °C. In an ELISA assay, an enzyme with a capture antibody adheres to the walls of the well plate, a sample with the analyte is introduced and the analyte binds to the antibody, a detection enzyme is bound to the analyte, the plate is washed to remove any unbound sample, then a chromogen is introduced. The well plate is then read with a plate reader at the peak wavelength of the chromogen (412 nm for our assay) and the emission intensity, where a higher intensity corresponds to a higher concentration of the analyte. We used

the 17(S)-Resolvin D1 ELISA assay to quantify the amount of Resolvin D1 released from the microgels into the supernatant at each timepoint to determine the timeline of release.

In Vivo Resolvin D1 Treatment

Non-Invasive Anterior Cruciate Ligament Injury

Preoperative care included anesthetizing the Male Lewis rats with isoflurane, injecting a weight-normalized dose of subcutaneous buprenorphine, and applying eye lubricant. Once sufficiently under anesthesia, the animals were transferred to the Non-Invasive Knee Injury (NIKI) device. The NIKI device applies an axial force to the left hind knee until ACL rupture occurs. After the injury, the animal was transferred to a recovery cage to wake up and then returned to their home cage. All studies were conducted under IACUC-approved protocols. Early OA pathology develops by 4 weeks post-injury and progresses to severe pathology by 8 weeks post-injury.

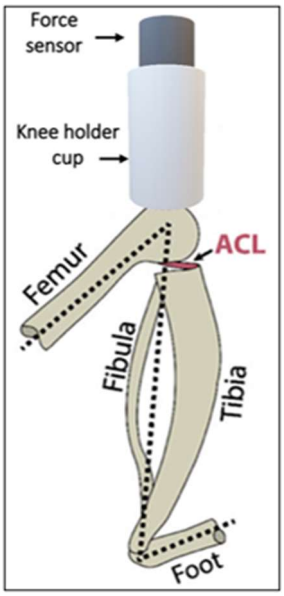

Figure 6: Anterior cruciate ligament injury schematic.

Resolvin D1 Administration

Animals were anesthetized with isoflurane then injected into the rear left knee joint with 30 µL of either saline solution (Sham, n=6), free drug (RvD1 (100 ng), n=3), or microgels solubilized in BSA (RvD1+Gel, n=3) depending on their group assignment. The animal was transferred to a recovery cage to wake up, then moved back to their home cage.

Bioseb Dynamic Weight Bearing

Bioseb Dynamic Weight Bearing (DWB) is a glass enclosure with a pressure plate that assesses how the animal spontaneously distributes their weight across their four limbs. DWB quantifies the functional therapeutic effects of our treatment groups compared to free drug and saline controls. The DWB assay was performed prior to injury to act as a baseline then once a week over the course of the study. We compared the mean percentage of weight bore on the injured limb over time to assess the ability of the treatment to act prophylactically to modify disease progression.

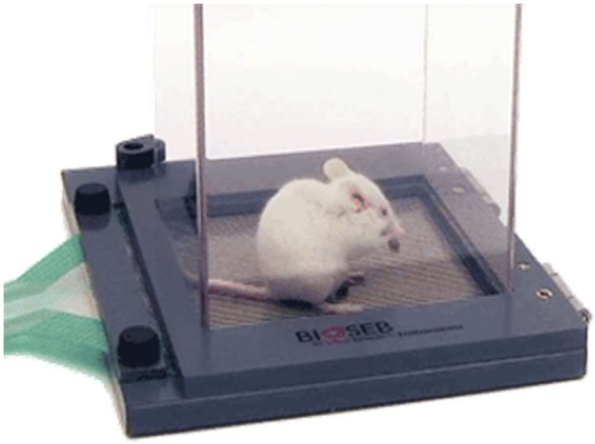

Figure 7: Bioseb Dynamic Weight Bearing enclosure.

microCT Imaging

Imaging of the animals' tibial plateau and femoral condyle of the injured joint allows for morphometric analysis and quantification of injury-induced cartilage degradation. After dissection, the animals' tibiae and femora were stored in phosphate buffer solution (PBS) and submerged in Conray contrast reagent for 30 minutes prior to imaging. One at a time, the tibiae and femora were transferred to a sealed sample chamber and then scanned using Scanco μCT 40. The raw scan data was reconstructed to 2D greyscale tomograms and then transposed orthogonally to produce coronal sections. When analyzing the effect of injury on cartilage in the knee joint, three metrics are analyzed: cartilage volume, cartilage thickness, and cartilage attenuation. Cartilage attenuation is a proxy for cartilage quality, where a higher cartilage attenuation value means that the cartilage is less healthy.

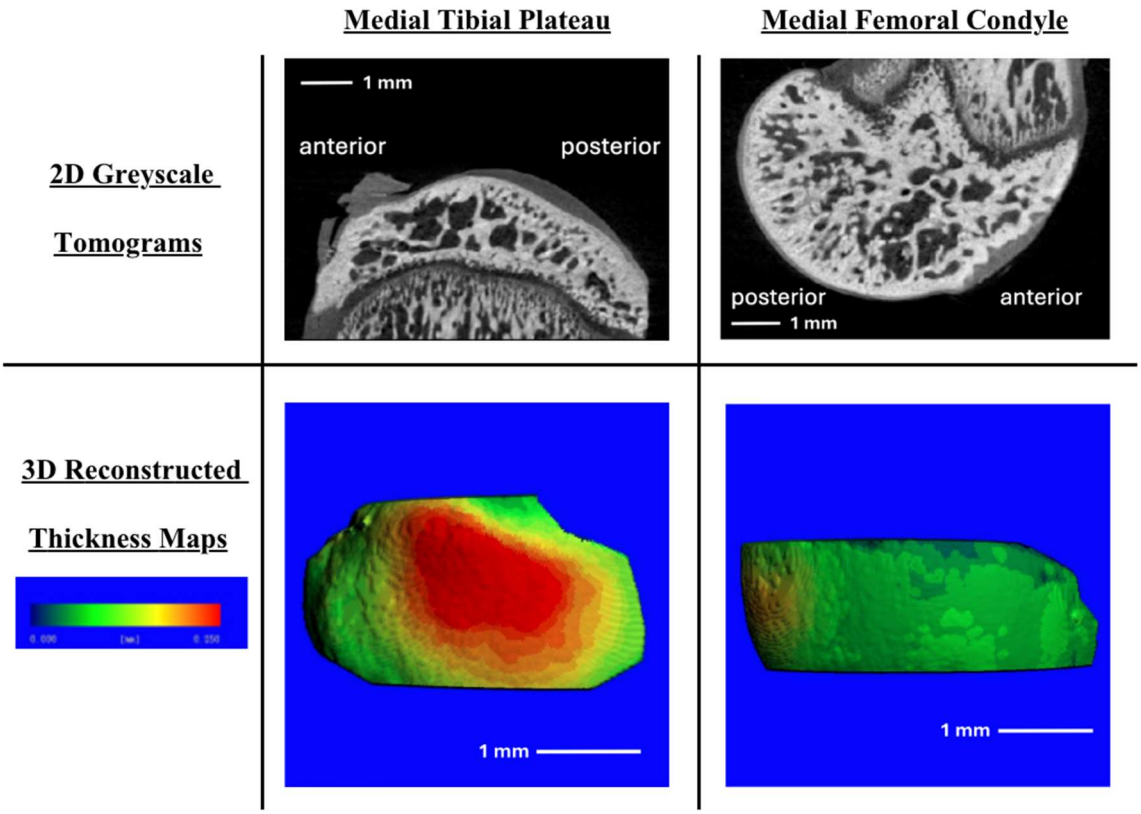

Figure 8: 2D greyscale tomograms and corresponding 3D reconstructed thickness maps for medial tibial plateau and medial femoral condyle of uninjured animal. Thickness map scale ranges from 0.000 to 0.250 mm.

Data Analysis

GraphPad Prism was used to graph data and determine statistical significance between groups using a mixed-effects ANOVA with Tukey's post hoc test ($p<0.05$). TNF-α staining data were analyzed with the Robust Regression Outlier Test (ROUT) to identify outliers with a Q = 1%. Igor64 was used to graph ELISA absorbance data.

Results and Discussion

In Vitro Resolvin D1 Characterization

Intracellular TNF-α Staining

Three low dose (5 ng/mL, 10 ng/mL, and 50 ng/mL) and one high dose (50 ng/mL, 100 ng/mL, and 500 ng/mL) Resolvin treatment staining protocols were completed. After the staining protocol was completed for low dose Experiment 3 and the high dose experiment, the cells were visualized on the fluorescent microscope, and it was noted that the DAPI stain was dimmer than expected, and the TNF-α stain could not be seen. It was deduced that the permeabilization step failed so the protocol was rerun on the same cells minus the blocking step and DAPI stain. The cells were then imaged, and the stains were visible in the proper channels.

We hypothesized that LPS stimulation would increase TNF-α production and for RvD1 treatment to attenuate TNF-α production.[8,13] In the representative images of our low and high dose experiments shown below (Figure 8 and 9), there was a clear visual increase of TNF-α stain from the unstimulated to stimulated groups. There was no obvious qualitative visual difference in the TNF-α stain with Resolvin D1 treatment across stimulated and unstimulated conditions.

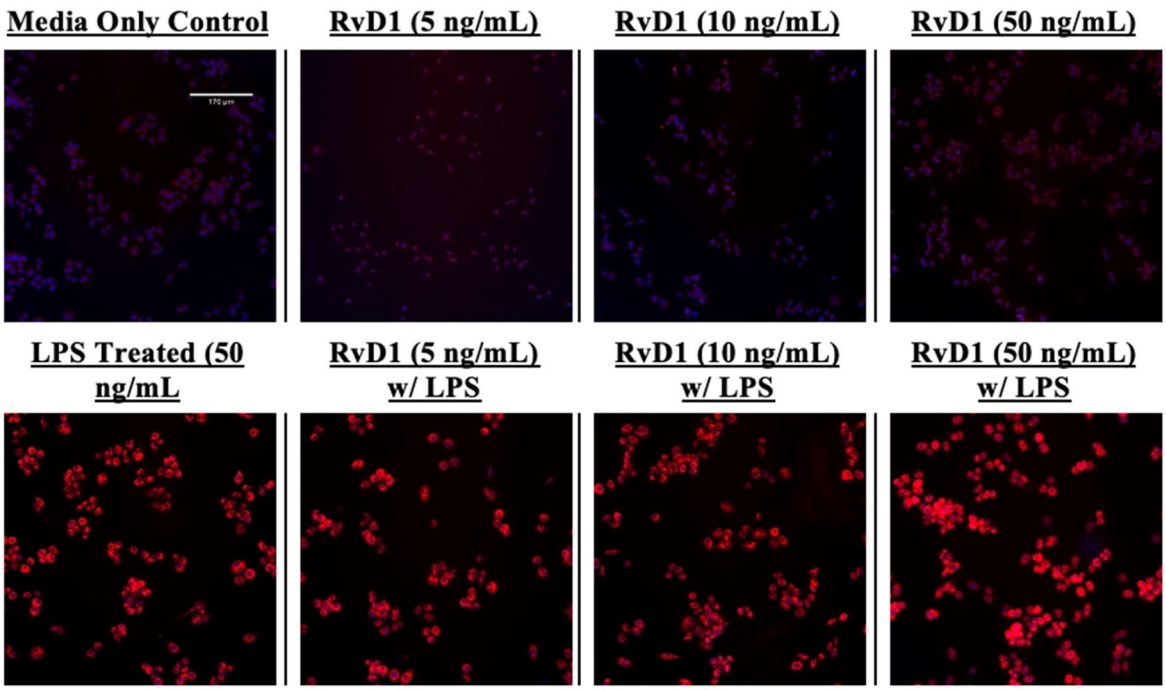

Figure 9: Intracellular TNF-α staining macrophage stimulation experiment, representative images (low dose RvD1 treatment). Blue = DAPI Nuclei Stain, Red = TNF-α Stain. Scale bar = 170 μm.

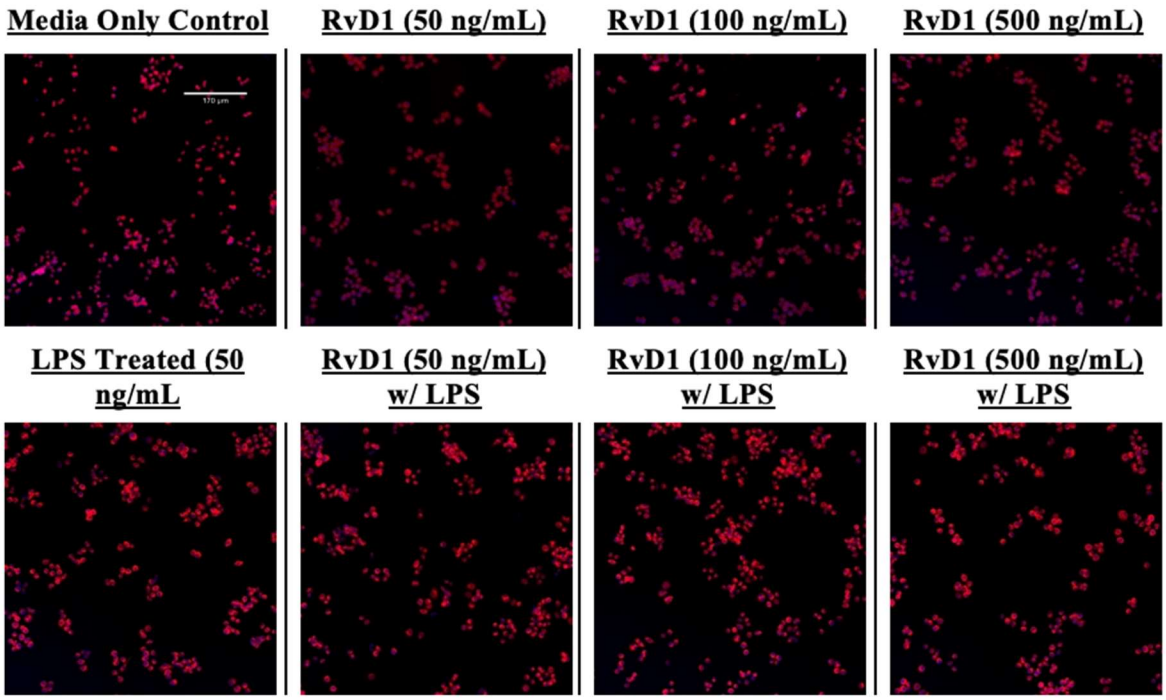

Figure 10: Intracellular TNF-α staining macrophage stimulation experiment, representative images (high dose RvD1 treatment). Blue = DAPI Nuclei Stain, Red = TNF-α Stain. Scale bar = 170 μm.

The % Area/nuclei and Mean Grey/nuclei data for Low Dose Experiments 1-3 were normalized to the Media Only control group then combined (Figure 10). The % Area/nuclei and Mean Grey/nuclei values exhibit the same clear trends, a strong significant increase in TNF-α production with LPS stimulation. There was no clear attenuation of TNF-α production with RvD1 treatment in either the stimulated or unstimulated groups. Further work is needed to determine why RvD1 did not attenuate TNF-α production as expected.

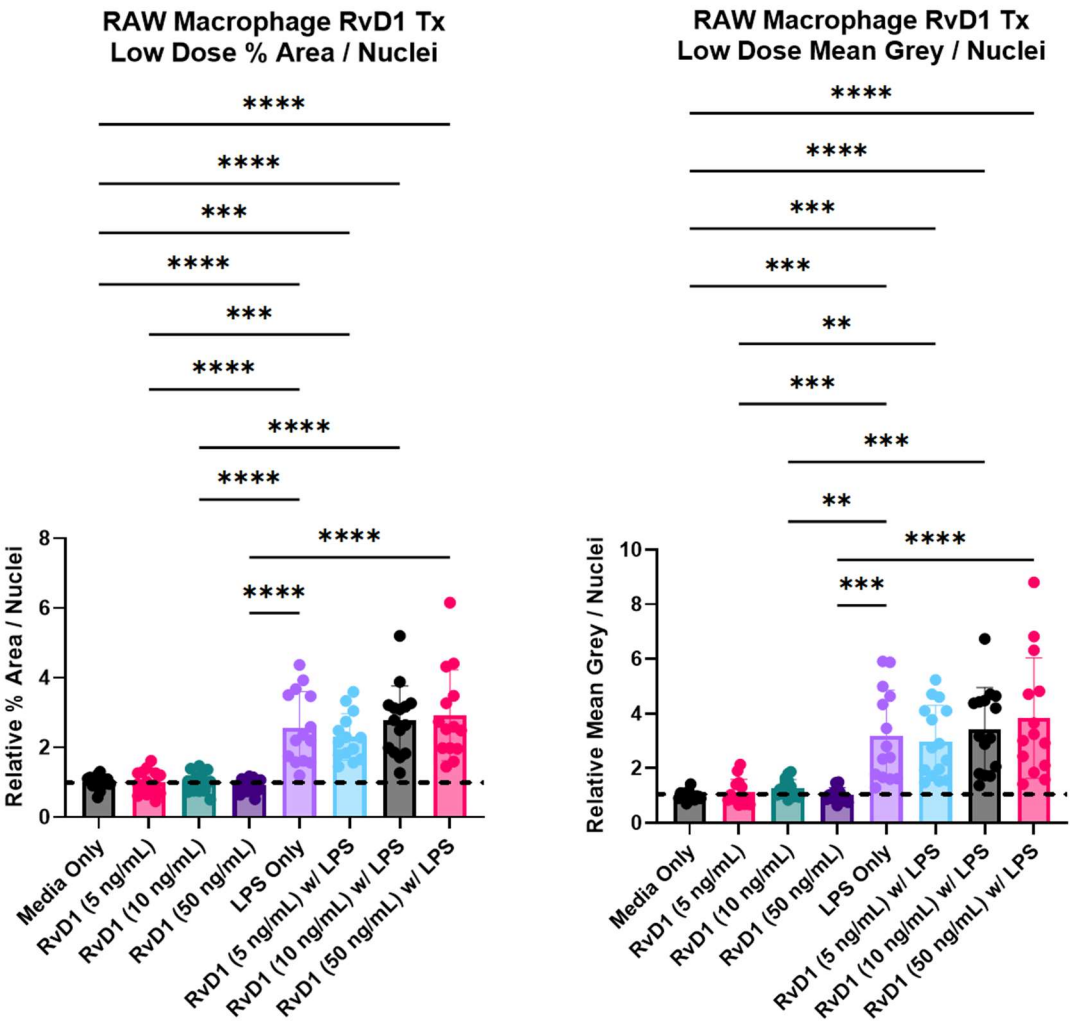

Figure 11: Percent area of TNF-α stain to image area normalized to nuclei count for triplicate low RvD1 dose macrophage treatment normalized to the Media Only control for Low Dose Experiments 1-3 (left). TNF-α stain intensity with subtracted background normalized to nuclei count for triplicate low RvD1 dose macrophage treatment normalized to media only control for Low Dose Experiments 1-3 (right). Dashed line at y=0. Significance of RvD1 of dose versus RvD1 w/ LPS of a different dose not shown on graph.

In our high dose staining experiment, there was no significant difference in the % Area/nuclei values between the stimulated and unstimulated groups. The Mean Grey/nuclei graph indicated a significant difference between the highest Resolvin dose (500 ng/mL) stimulated group and its unstimulated counterpart as well as the Media Only control; there was

no significance denoted between other stimulated and unstimulated groups. It was unsurprising that the difference in TNF-α production was less apparent in these cells because they appeared to have a high basal level of TNF-α production in unstimulated conditions. This could be influenced by a variety of factors including passage number (e.g., how 'old' the cells are) and culture conditions when frozen/thawed for storage (e.g., the amount of cryoprotectant left with the cells during the thaw process). Since the unstimulated cells already had significant TNF-α production, the difference in area of the TNF-α stain was similar, but the intensity of the stain was visually increased, meaning that in this case, the Mean Grey/nuclei measure was more suitable. It is important to note that light exposure in the images, the background noise, and other factors affect the image analysis, and therefore either the % Area/nuclei or Mean Grey/nuclei may produce more consistent values depending on the experimental conditions.

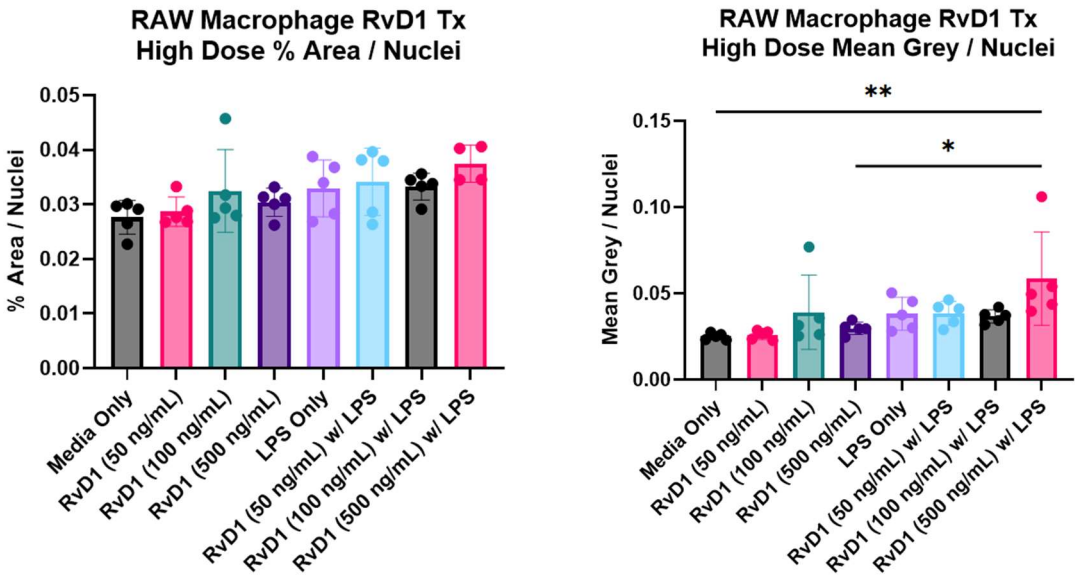

Figure 12: Percent area of TNF-α stain to image area normalized to nuclei count for high RvD1 dose macrophage treatment (left). TNF-α stain intensity with subtracted background normalized to nuclei count for high RvD1 dose macrophage treatment (right). Significance of RvD1 of dose versus RvD1 w/ LPS of a different dose not shown on graph.

Measure-It High Sensitivity Nitrite Quantization Assay

Since nitrite is produced in response to inflammation, it is anticipated that LPS stimulation would increase nitrite media concentration. We also expected RvD1 treatment to decrease nitrite media concentration as a regulator of inflammation. As seen in Figure 12, we detected no change in nitrite levels with LPS stimulation or RvD1 treatment at low or high doses. We have speculated that the Measure-It High Sensitivity Nitrite Quantization Assay may not have worked as intended. Other work in the Willett Lab using the same assay to quantify nitrite production in cytokine stimulation of synoviocytes also demonstrated no change, contrary to expectation. Since the nitrite standard curves for both the low and high dose experiments appeared as expected (linear with a y-intercept near zero), and we saw consistent fluorescence for a basal level of nitrite, we inferred that there is no issue with binding of the fluorophore to the

standard or nitrite in the media. Possible areas of improvement include seeding a higher cell density, decreasing the amount of media the cells grow in, and lysing the cells before media collection to more clearly see the difference in nitrite production between stimulated and unstimulated groups as well as treatment groups.

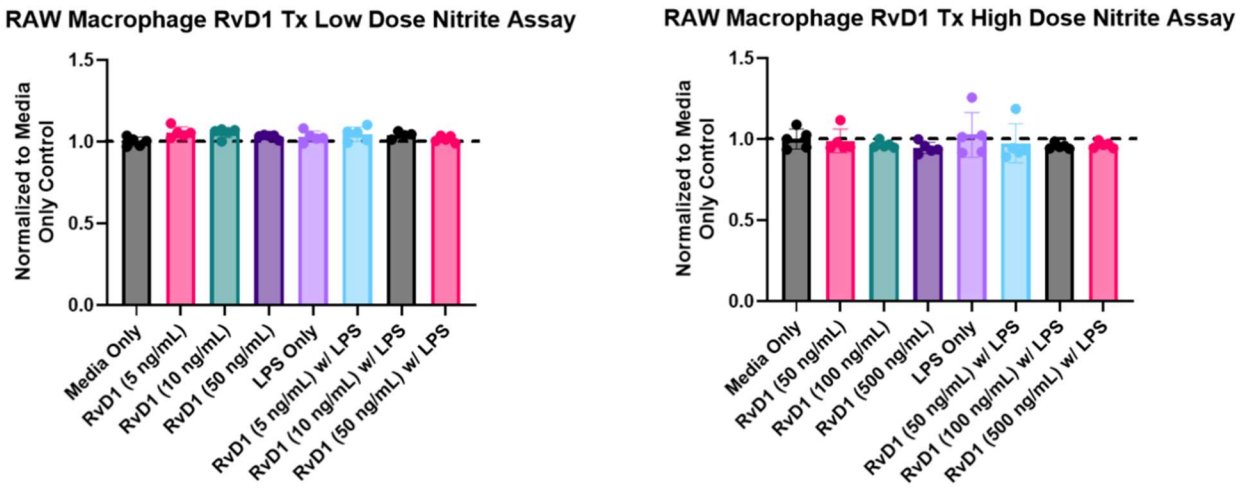

Figure 13: Nitrite content for low (left) and high (right) RvD1 macrophage treatment experiments, normalized to Media Only Control.

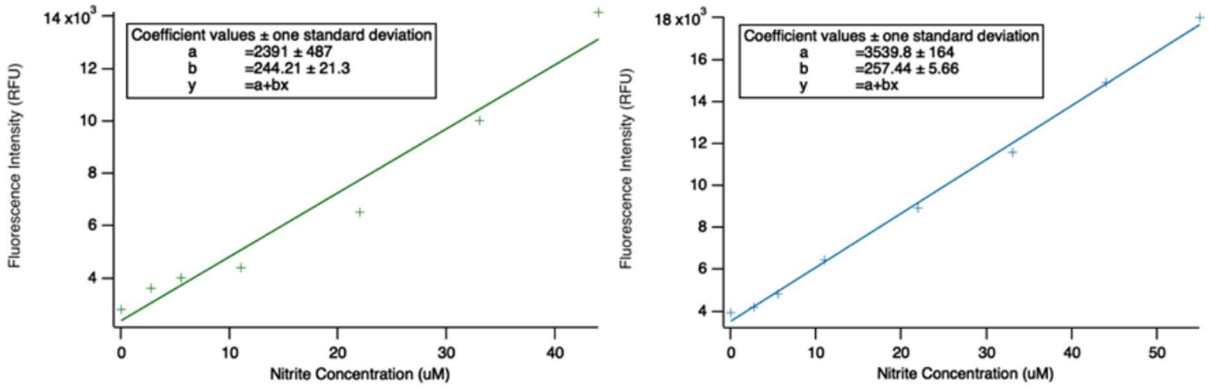

Figure 14: Nitrite standard curve for low (left) and high (right) RvD1 macrophage treatment experiments.

In Vitro Microgel Fabrication and Quantization

Enzyme Linked Immunosorbent Assay

We performed a timed-release assay to quantify the relative amount of RvD1 diffused from the PEG microgels into solution. We hypothesized that storing the gels at 4 °C would slow the release rate of RvD1 compared to storage at physiological 37 °C. At the 1-hour, 4-hour, and 18-hour timepoints, the absorbance values were very similar, suggesting that the storage temperature had little effect on the diffusion rate. Between 18 and 24 hours, there was a sharp decrease in absorbance; this is likely due to the hydrolysis of the hydroxides on the lipid chain of Resolvin D1 which prevents accurate characterization of the mechanism of drug release. A subsequent experiment should include a Resolvin D1-only control at the corresponding timepoints to allow for normalization to the amount of unhydrolyzed RvD1. A possible explanation for the difference in absorbance between the 4 °C and the 37 °C group at the 48-hour timepoint is that the cooler temperatures in the 4 °C group affected the hydrolysis of the Resolvin D1, recovering some to the original unhydrolyzed form.

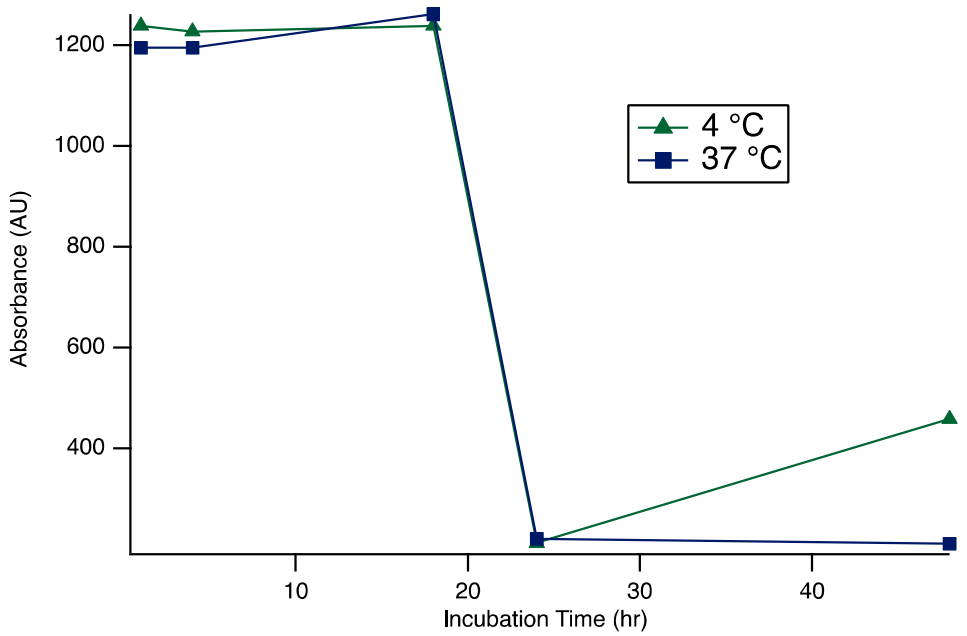

Figure 15: Absorbance of Resolvin D1 in isolated supernatant from microgel samples stored at 4 °C or 37 °C at 412 nm (n=1).

In Vivo Resolvin D1 Treatment

Bioseb Dynamic Weight Bearing

Bioseb Dynamic Weight Bearing was performed 1 week, 3 weeks, and 4 weeks post-injury. The values were normalized to the animals' pre-injury controls. At all timepoints, the animals bear less weight on their injured limb, both compared to their baseline levels and the Sham group. In Figure 16, we look at just the 4-week post-injury timepoint with the added injury-only group from historical data collected in the Willett lab (as a control); there is no available injury-only data for the 1-week and 3-week post-injury timepoints. The RvD1 treatment groups did not bear more weight on their injured limb compared to the untreated injury group. Any therapeutic effects that the Resolvin D1 has on injury pathology are not substantial enough to encourage greater weight bearing from either decreased pain or increased function, at

least at this timepoint. It is possible that at later stages of disease such as at 8-weeks post-injury, when we see more severe pathology, therapeutic effects would become more evident. Future work should investigate functional outcomes at later disease stages and the therapeutic effects resulting from either a higher dose of Resolvin D1, repeat injections of the drug to increase bioavailability, or a combination of both.

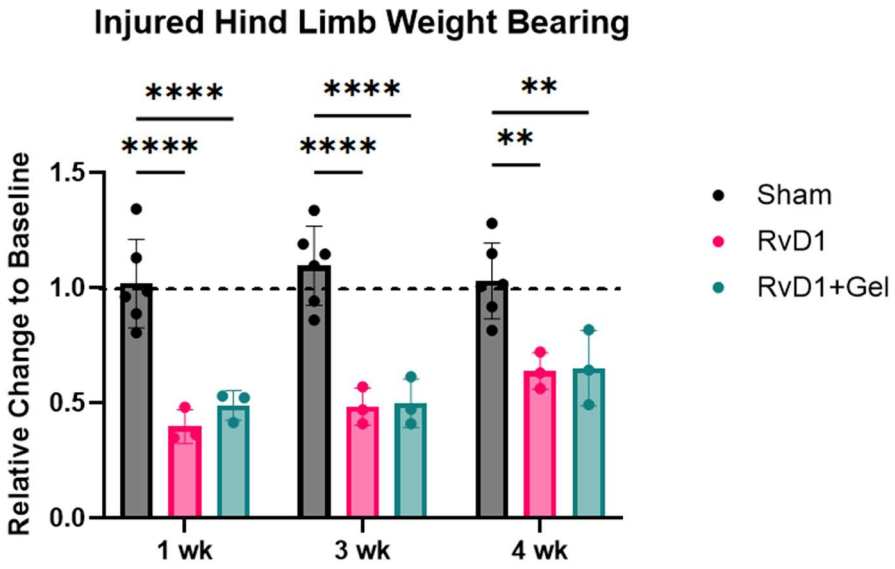

Figure 16: Injured hind limb weight bearing for Sham and free and encapsulated RvD1 treatments groups, 1 week, 3 weeks, and 4 weeks post-injury, normalized to baseline levels.

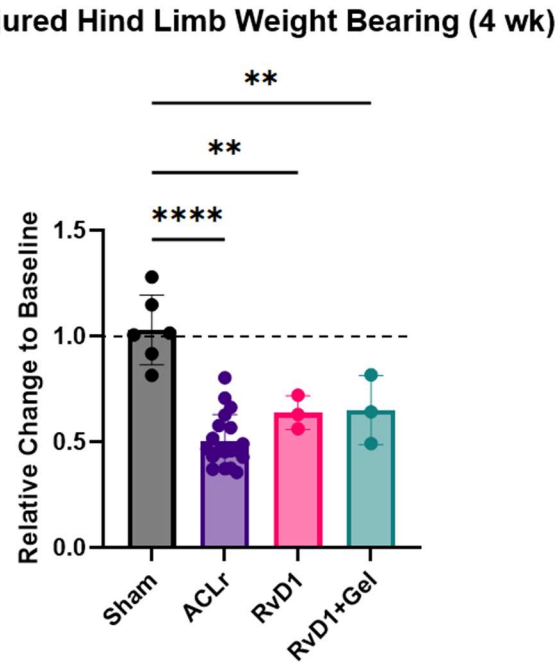

Figure 17: Injured hind limb weight bearing for Sham and free and encapsulated RvD1 treatments groups with added historical ACLr injury group data, 4 weeks post-injury, normalized to baseline levels.

microCT Imaging

Representative images of the treatment groups in Figure 17 show morphologies consistent with ACLr injury at the 4-week post-injury timepoint. There is a thickening in the cartilage of both the tibial plateau and femoral condyle compared to the Sham group. In the femur, there is a visible lesion in the cartilage. There seems to be increased cartilage thickening on the posterior side of the femoral condyle (left side of the image) in the treatment groups compared to ACLr injury alone. Previous work in the Willett lab has characterized the effect of ACLr injury on cartilage in the full medial plateau, medial 1/3 of the medial plateau, and full medial condyle. ACLr data in the following graphs are from the 4-week post-injury timepoint of the historical study.

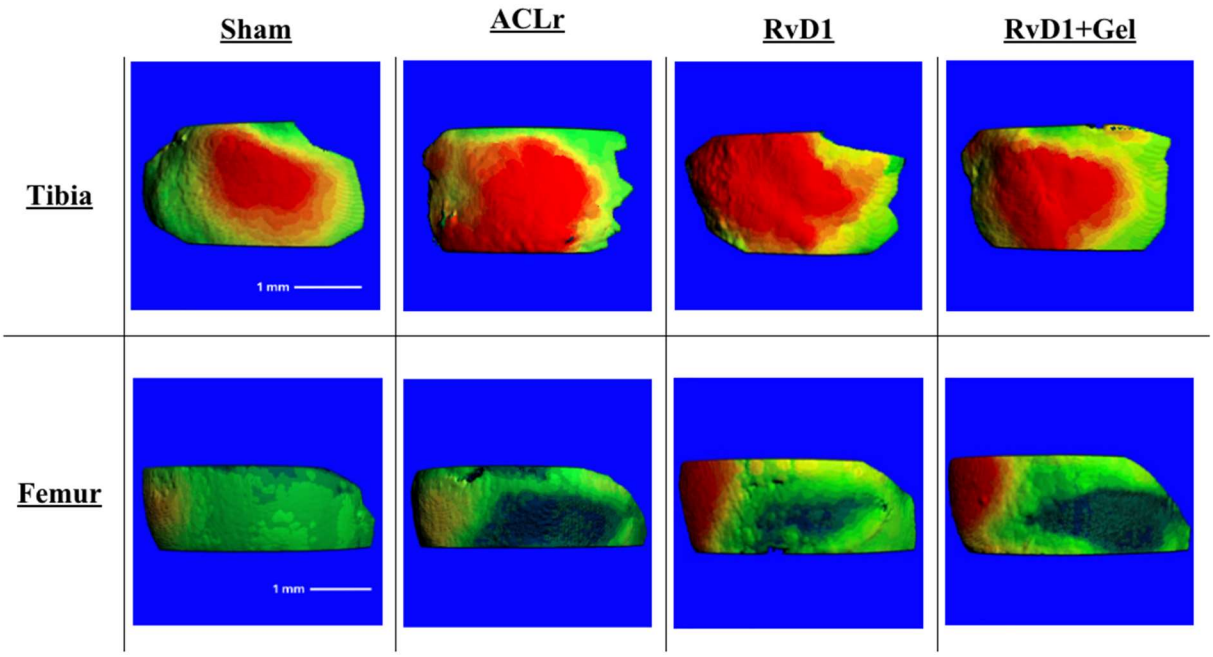

Figure 18: Representative 3D reconstructed thickness maps of medial tibial plateau and medial femoral condyle for Sham, RvD1, and RvD1+Gel groups, 4 weeks post-injury.

In general, we find that by isolating the medial 1/3 of the medial condyle, we can better quantify the morphological changes due to ACL rupture injury in the tibial cartilage. In the full medial cartilage, the RvD1+Gel group showed significantly increased cartilage volume compared to the injury-alone group (Figure 18). The RvD1+Gel group was not significantly different from the Sham group; however, the increased cartilage volume was not evidently associated with healthy or injury pathology (Figure 18). The difference in significance between the injury group and the encapsulated and unencapsulated groups may be due to differences in the release profile of the RvD1 (Figure 18). In the medial 1/3, the RvD1+Gel group exhibited significantly increased cartilage thickness compared to both the Sham and ACLr groups (Figure 19). As cartilage volume and thickness are related, the finding that the RvD1+Gel group differs from both the non-injury and injury controls suggests that the treatment has a morphological

effect on the cartilage, possibly independent of changes due to injury. Again, it is important to note that this same discrepancy is not evident in the free RvD1 group (Figure 19). In the medial 1/3, the ACLr injury group has significantly increased cartilage attenuation compared to the Sham group, while the treatment groups were not significantly different from Sham; this suggests that the RvD1 treatment may help preserve the glycosaminoglycan content in the cartilage (i.e., an improved cartilage quality) (Figure 19). The RvD1+Gel group however did not significantly differ from the ACLr group, indicating that the microgels may slightly impede the therapeutic effects of the RvD1 as opposed to enhance as we expected (Figure 19).

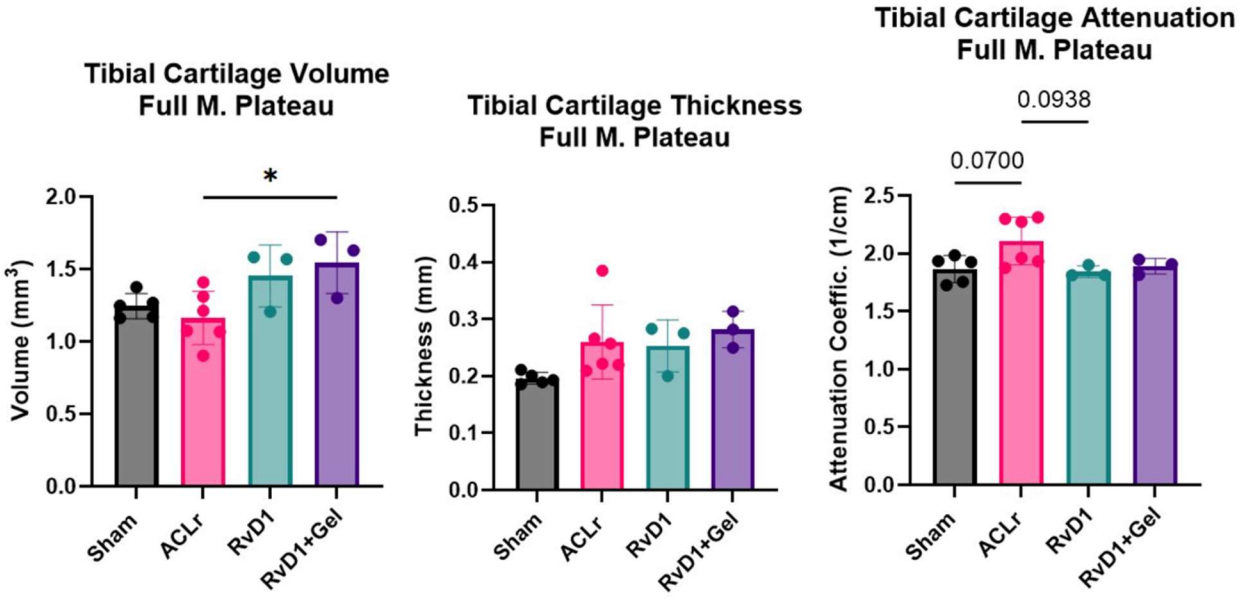

Figure 19: Cartilage volume (left), cartilage thickness (middle), and cartilage attenuation (right) for full medial plateau of back left tibia, 4 weeks post-injury. Significance denoted as number if 0.1>p>0.5.

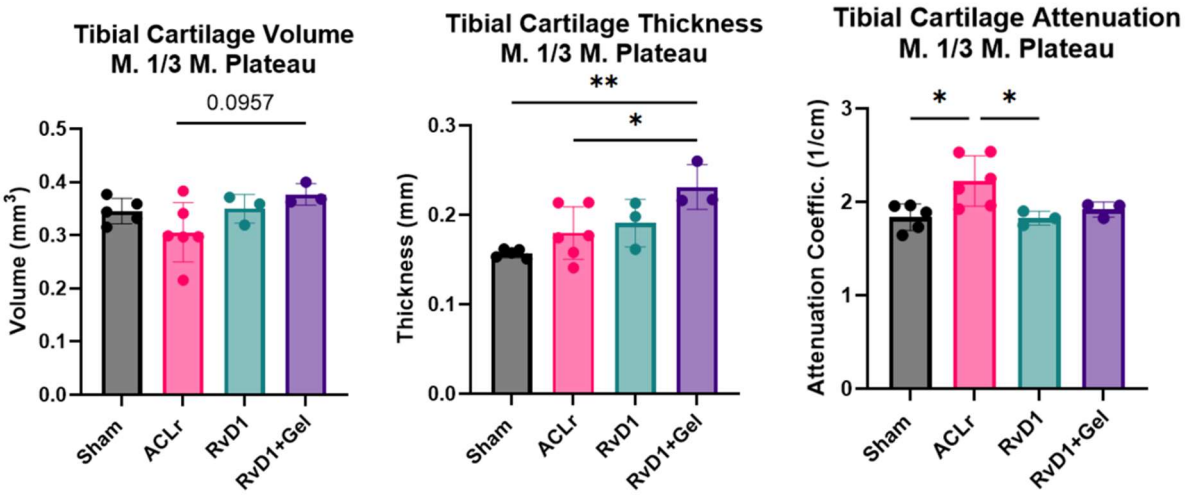

Figure 20: Cartilage volume (left), cartilage thickness (middle), and cartilage attenuation (right) for medial 1/3 of the medial plateau of back left tibia, 4 weeks post-injury. Significance denoted as number if 0.1>p>0.5.

In the femoral cartilage, there is evidently no effect of either injury or treatment on the cartilage volume or attenuation. Interestingly, there was an increase in cartilage thickness in both treatment groups compared to both the Sham and ACLr groups. Increased cartilage thickness in the full medial condyle is associated with ACLr injury morphology, but the treatment appears to have exacerbated the pathology; this corroborates what the representative images show. Since both the free and encapsulated groups exhibit this effect, it is reasonable to conclude that the RvD1 impacted the physiology of the joint in some unanticipated way.

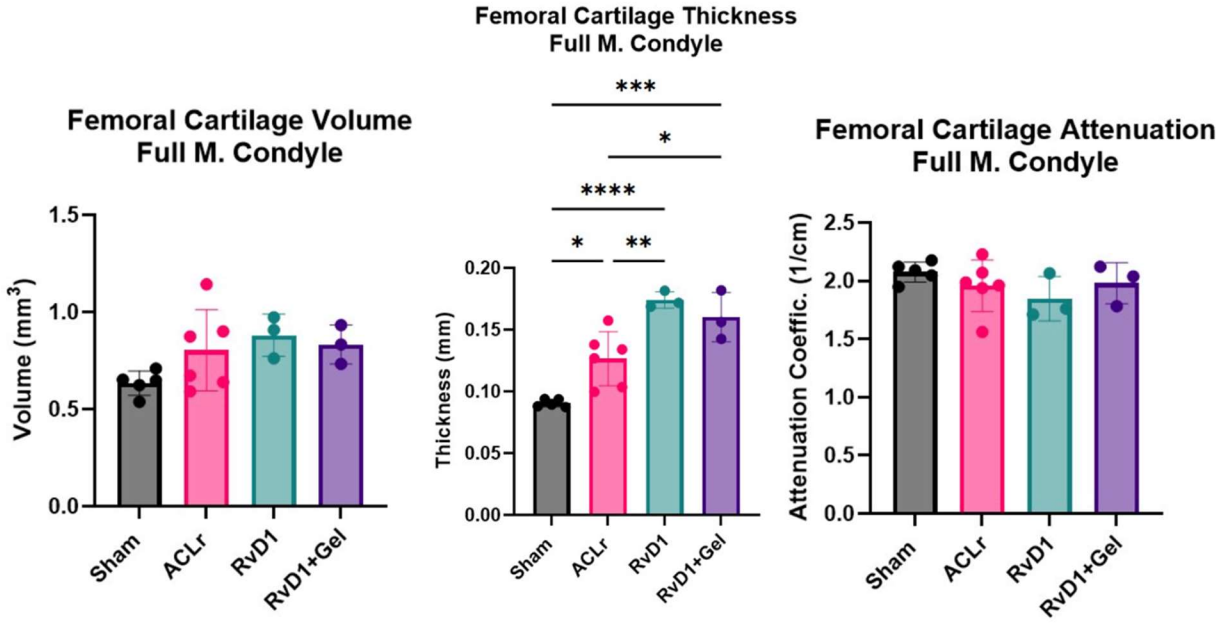

Figure 21: Cartilage volume (left), cartilage thickness (middle), and cartilage attenuation (right) for full medial condyle of back left femur, 4 weeks post-injury.

Conclusion

This work aimed to characterize Resolvin D1 both *in vitro* and *in vivo* for the treatment of osteoarthritis pathology. We hypothesized that Resolvin D1 would (1) attenuate the production of TNF-α and nitrite (markers of inflammation) in macrophages and (2) decrease ACLr-induced functional and morphological pathologies with an improved therapeutic effect when encapsulated in polyethylene glycol microgels.

In vitro experiments were inconclusive; TNF-α staining confirmed that LPS stimulation increases TNF-α production, but RvD1 treatment did not decrease TNF-α production at any dose when either stimulated or unstimulated. Future experiments will investigate TNF-α production in a different cell line of macrophages. The nitrite quantization assay showed no change in nitrite concentration with LPS stimulation or RvD1 treatment; future directions involve measuring nitrite content via a different method. From prior research in the field, we expect Resolvin D1 to be anti-inflammatory, meaning that it should decrease markers of inflammation such as TNF-α and nitrite; further work is needed to elucidate why our findings contradict those of the field.

In vivo, we see no difference in functional outcomes between injury alone and treatment groups. The therapeutic effects of Resolvin D1 treatment may be improved by increasing treatment dose or administering repeat injections. Regarding morphological outcomes, the encapsulated RvD1 group minorly increased tibial cartilage volume compared to the injury alone group and increased tibial cartilage thickness compared to both the injury and non-injury controls. Both RvD1 treatment groups increased femoral cartilage thickness compared to injury and non-injury controls. These findings suggest that both the Resolvin D1 and PEG microgels affect knee joint cartilage in ways other than just attenuating injury pathology. A fully powered study is needed to corroborate these findings. The chronic inflammation associated with

osteoarthritis is known to be a driving factor of the disease; as such, we expect the introduction of an anti-inflammatory agent such as Resolvin D1 to attenuate disease pathology. A sustained-release drug delivery vehicle such as PEG microgels should increase the bioavailability of Resolvin D1, thereby enhancing therapeutic effects. Further work is needed to verify the efficacy of Resolvin D1 as a disease-modifying therapeutic for the treatment of OA.

Overall, Resolvin D1 is a promising candidate for the treatment of osteoarthritis, but much more extensive research is needed to validate the efficacy of the treatment in practice. The road to clinical application is a long one; following positive conclusive findings *in vitro* and in a small animal model, such as our murine preclinical injury model, Resolvin D1 would move onto large animal studies and finally into clinical studies. The early evaluative work we do is essential for identifying potential treatments for diseases such as osteoarthritis that severely impact quality of life yet very limited treatment options.

Bibliography

1. Kotlarz, H.; Gunnarsson, C. L.; Fang, H.; Rizzo, J. A. Insurer and Out-of-Pocket Costs of Osteoarthritis in the US: Evidence from National Survey Data. Arthritis & Rheumatism 2009, 60 (12), 3546–3553. https://doi.org/10.1002/art.24984.

2. Alinezhad, H.; Daloii, A. A.; Farzanegi, P.; Abdi, A. Comparing the Effects of Regular Aerobic Training, Hyaluronic Acid, and Mesenchymal Stem Cells on Wnt/β-Catenin Signaling of Cardiac Tissue in Rats with the Experimental Model of Knee Osteoarthritis. *J Arch Mil Med* **2022**, *10* (2). https://doi.org/10.5812/jamm-122228.

3. Constantino de Campos, G.; Mundi, R.; Whittington, C.; Toutounji, M.-J.; Ngai, W.; Sheehan, B. Osteoarthritis, Mobility-Related Comorbidities and Mortality: An Overview of Meta-Analyses. *Ther Adv Musculoskelet Dis* **2020**, *12*, 1759720X20981219. https://doi.org/10.1177/1759720X20981219.

4. Jack, K.; McLean, S. M.; Moffett, J. K.; Gardiner, E. Barriers to Treatment Adherence in Physiotherapy Outpatient Clinics: A Systematic Review. *Man Ther* **2010**, *15* (3–2), 220–228. https://doi.org/10.1016/j.math.2009.12.004.

5. Ji, R.-R.; Xu, Z.-Z.; Strichartz, G.; Serhan, C. N. Emerging Roles of Resolvins in the Resolution of Inflammation and Pain. Trends Neurosci 2011, 34 (11), 599–609. https://doi.org/10.1016/j.tins.2011.08.005.

6. Dravid, A. A.; M. Dhanabalan, K.; Agarwal, S.; Agarwal, R. Resolvin D1-loaded Nanoliposomes Promote M2 Macrophage Polarization and Are Effective in the Treatment of Osteoarthritis. Bioeng Transl Med 2022, 7 (2), e10281. https://doi.org/10.1002/btm2.10281.

7. Taciak, B.; Białasek, M.; Braniewska, A.; Sas, Z.; Sawicka, P.; Kiraga, Ł.; Rygiel, T.; Król, M. Evaluation of Phenotypic and Functional Stability of RAW 264.7 Cell Line through Serial Passages. *PLoS One* **2018**, *13* (6), e0198943. https://doi.org/10.1371/journal.pone.0198943.

8. Meng, F.; Lowell, C. A. Lipopolysaccharide (LPS)-Induced Macrophage Activation and Signal Transduction in the Absence of Src-Family Kinases Hck, Fgr, and Lyn. *J Exp Med* **1997**, *185* (9), 1661–1670.

9. Yusuf, A.; Almotairy, A. R. Z.; Henidi, H.; Alshehri, O. Y.; Aldughaim, M. S. Nanoparticles as Drug Delivery Systems: A Review of the Implication of Nanoparticles' Physicochemical Properties on Responses in Biological Systems. *Polymers (Basel)* **2023**, *15* (7), 1596. https://doi.org/10.3390/polym15071596.

10. Li, X.; Dai, B.; Guo, J.; Zheng, L.; Guo, Q.; Peng, J.; Xu, J.; Qin, L. Nanoparticle–Cartilage Interaction: Pathology-Based Intra-Articular Drug Delivery for Osteoarthritis Therapy. *Nano-Micro Lett.* **2021**, *13* (1), 149. https://doi.org/10.1007/s40820-021-00670-y.

11. Mancipe Castro, L. M.; Sequeira, A.; García, A. J.; Guldberg, R. E. Articular Cartilage- and Synoviocyte-Binding Poly(Ethylene Glycol) Nano-Composite Microgels as Intra-Articular Drug Delivery Vehicles for the Treatment of Osteoarthritis. *ACS Biomater Sci Eng* **2020**, *6* (9), 5084–5095. https://doi.org/10.1021/acsbiomaterials.0c00960.

12. Li, L.; Asteriou, T.; Bernert, B.; Heldin, C.-H.; Heldin, P. Growth Factor Regulation of Hyaluronan Synthesis and Degradation in Human Dermal Fibroblasts: Importance of Hyaluronan for the Mitogenic Response of PDGF-BB. *Biochem J* **2007**, *404* (Pt 2), 327–336. https://doi.org/10.1042/BJ20061757.

13. Xiang, S.; Ye, Y.; Yang, Q.; Xu, H.; Shen, C.; Ma, M.; Jin, S.; Mei, H.; Zheng, S.; Smith, F.; Jin, S.; Wang, Q. RvD1 Accelerates the Resolution of Inflammation by Promoting Apoptosis of the Recruited Macrophages via the ALX/FasL-FasR/Caspase-3 Signaling Pathway. *Cell Death Discov.* **2021**, *7* (1), 1–10. https://doi.org/10.1038/s41420-021-00708-5.